Landslide Hazard Zonation of Tehri Reservoir Rim Area Using Modified LHEF Rating Scheme

Rohan Kumar[1*], Rathinam Anbalagan[2], Ankita Agarwal[3], K Khusulio[4]

[1*] Department of Chemical and Petroleum Engineering, School of Chemical Engineering and Physical Sciences, Lovely Professional University, India
[2]Departement of Earth Sciences, IIT Roorkee, India
[3]Departement of Chemical and Petroleum Engineering, School of Chemical Engineering and Physical Sciences, Lovely Professional University, India
[4]Departement of Chemical and Petroleum Engineering, School of Chemical Engineering and Physical Sciences, Lovely Professional University, India

*Corresponding author : rohan25322@lpu.co.in

Abstract: The study aimed to utilize the capabilities of geospatial technology for landslide hazard evaluation factor (LHEF) scheme recorded in the Bureau of Indian Standard (BIS) code to prepare a landslide hazard zonation (LHZ) map of the Tehri reservoir rim area at the macro-scale. Multisource remote sensing data were visually and digitally interpreted to produces thematic layers and slope facet as recorded in BIS method. LHEF method is suited for meso and macro scale mapping thus, to broaden the scope of LHEF scheme, novel approaches were adopted namely, the mapping unit 'slope facet' was more precisely extracted through digital and visual interpretation of remote sensing data, the structural favorability map was extracted using photo-lineament density criteria. Additionally, two external factors, rainfall and seismicity were incorporated in LHEF rating scheme and used a matrix-based system to propose their combined rating. With the modified LHEF rating scheme, we have succeeded in identifying LHZ with reasonable accuracy. The bar chart method used to validate LHZ results that clearly indicated a high number of landslides falling in high to very high hazard zone conversely, very few landslides observed in low to very low hazard zone identified from current approach.

Keywords: Landslide hazard zonation, Landslide hazard evaluation factor, Tehri reservoir, slope facet

1. Introduction

In the last few decades, the number of disaster events has sharply increased. Approximately, 15% of the Indian landmass prone to landslides (GSI, http://www.portal.gsi.gov.in) which includes the vast terrain of the Himalaya, Nilgiris and Western Ghat. Factors affecting the landslides in the Himalayan region are steep slope angle, fragile slope material, peculiar structural discontinuities, large-scale anthropogenic activities, cloud bursts, etc. In the recent past, dams, reservoirs, tunnels, road networks, hydroelectric power plants, and townships have come up in a big way in the fragile Himalayan terrain. Along with the positive side of the development work, there are some major challenges related to sustainability since a number of slope failures and land subsidence are reported during and after such development works. This work deals with landslide propensity assessment on the slopes bounding 70-kilometer-long Tehri reservoir.

The construction of a 260-meter-high Tehri Dam at the confluence of the Bhagirathi and Vilangana Rivers, situated in the highly rugged Lesser Himalayan terrain formed the Tehri reservoir. Between monsoon and summer, reservoir water fluctuates from el ± 830 m (maximum reservoir level) to el ± 740m (dead storage level), thus creating a drawdown of roughly 90m that leads to a number of slope failures in the reservoir rim. The combination of the intrinsic property of the terrain and the drawdown condition has put serious stress on villages, agricultural lands, road networks, forest land, and other infrastructure situated on the slopes bounding the reservoir. Therefore, there is an eminent need for landslide mitigation in the reservoir rim region.

Landslide Hazard Zonation (LHZ) mapping is an initial step towards landslide hazard mitigation. On the basis of a set of geo-environmental factors, LHZ mapping identified the landslide probable zones [1-2] and founded that the set of conditions which were responsible for past and present landslides will likely induce future landslides. Presently, LHZ mapping is carried out using heuristic [3-6], probabilistic/statistical methods [7-10], semi-quantitative/logical [11-13], deterministic or physically based [14-15] and machine learning methods [16-19]. An exhaustive literature survey has indicated the relative potential of each method of LHZ mapping, in addition to many gaps. While the heuristic method is based on the subjective judgement of professionals, statistical, probabilistic, or machine learning methods have a very high influence on training data and hence produce a biased estimate of the hazard zone. An important gap has been identified in the form of mapping unit selection. In the majority of work, raster grids have been selected as mapping units that have a major reliability issue. In this study, the capability of the landslide hazard evaluation factor (LHEF) scheme recorded in Bureau of Indian Standard (BIS) guidelines (IS : 14496 Part-2 1998) was used for identifying relative landslide hazard zones. From an engineering geological perspective, the LHEF rating scheme, an empirical approach best fits the heuristic model. This approach is adopted by BIS for practicing LHZ mapping in the hilly terrains of India at the meso-scale (1:5000 – 1:10000) and macro-scale (1:25000 - 1:50000). It assumes the gross influence of the following six causative geo-environmental factors: slope morphometry, relative relief, lithology, structural favorability, hydrogeological condition, and LULC. These fixed ratings are relative ratings (varying according to the sub-categories of factors), and they do not require landslide incidences as an input, so they do not produce biased estimates. One of the important inputs to the LHEF scheme is the ‘uniform terrain unit called slope facet’. Slope facet is a terrain unit having similar slope characteristics and is bordered by natural features such as streams, ridges, spars, depressions, etc. The slope facet is a more practical and reliable mapping unit compared to the grid, so the ultimate LHZ map will have better applicability compared to other methods. A number of authors have used the LHEF rating scheme for LHZ mapping at different scales [3, 20-24]. A noticeable gap was found in the quality of the input data, mainly due to the scale of the mapping. In this work, a novel approach was adopted to extract quality input data that would produce a practical LHZ map. Government agencies can easily use this LHZ map for landslide hazard mitigation purposes.

1.1 Study Area

The Tehri reservoir rim area, the area bounding the reservoir is located in the highly surge terrain of the Lesser Himalaya (Fig: 1). The reservoir bounded by moderate to steep slopes support settlements, forest land, crop land, etc., and thus represented by cliffs, ridges, spurs, deeply dissected valleys, well-developed terraces, and abrupt, sharp slopes. Ridges and spurs are occupied by dense or sparse forests whereas moderate slopes are generally supported by agricultural lands, plantations, and settlements. The area is drained by typical mountainous drainage patterns such as parallel, sub-parallel, and sub-dendrite. 70-kilometer-long reservoir is filled during the monsoon season and dry substantially in the summer season, thus creating a drawdown condition. The reservoir drawdown takes place between the maximum reservoir level (MRL 830m) and the dead storage level (DSL 740m). When the reservoir attains MRL, it saturates the bounding slopes, and when the water level goes down, saturated valley slopes attain instability at a number of places. Instability on the bounding slopes depends on the following factors: (i) the nature of the slope-forming material; (ii) slope geometry; (iii) vegetation support on the slopes; and (iv) anthropogenic activity along the reservoir. Reservoir water fluctuation leads to various instability problems, and these are manifested in terms of landslides, subsidence, sinkholes, etc. Typical arcuate-shaped landslides (also called reservoir-induced landslides), which originate at reservoir level, have been found progressing at the upper reaches of the slopes and encroaching settlements. Additionally, roads have been constructed by randomly cutting the reservoir-bounding slopes, and this has only aggravated the instability problem in the reservoir rim area.

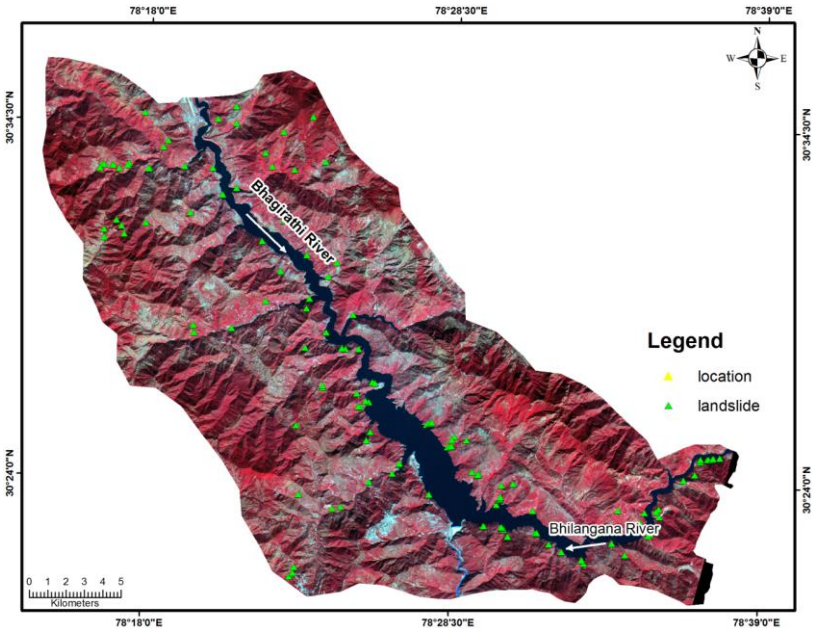

Figure 1: Map highlighting Tehri reservoir area

1.2 **Landslides of Tehri reservoir rim area**

Landslides were observed through field visits, historical information, and the analysis of high-resolution satellite data. Worldview-2 PAN and VNIR, LISS-IV VNIR, and Sentinel-2 VNIR imageries of different years were analyzed for the identification of landslides. Landslides from the images were extracted using the following visual interpretation techniques: shape, contrast, pattern, and association. Landslides in the area can be grouped into the following categories: debris slide, debris slump, rock slide, and complex landslide. A vast number of the slopes bounding the reservoir are formed of loose materials such as RBM and debris. Debris slide and debris slump have been observed in such slope-forming materials (Fig. 2a–d). A series of landslides were observed along the road network that were mainly caused by the unplanned slope cutting required for road construction (Fig. 2 e–f). Many landslides were observed directly connected to the reservoir (Fig. 2g–h).

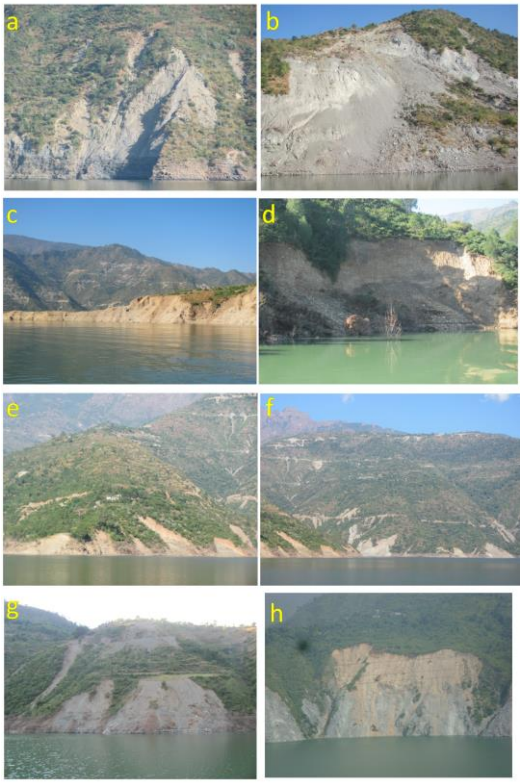

Figure 2 Landsides observed during field observations; a-d: Landslides in loose slope forming materials, e-f: series of landslides initiated due to road cut, g-h: reservoir induced landslides

2. Materials and Methods

2.1 Data used

As per the LHEF scheme of BIS (Code: IS 14496 Part 2), landslide-causing factors were acquired and derived through various sources, such as the Survey of India topographic map (1:25,000 scale), the geological map prepared by Valdiya [25], the satellite sensors LISS IV, Sentinal-2, and Worldview-2 (multispectral/PAN data), and the ALOS PALSAR 12.5m digital elevation model (DEM) (Table 1). The processing of remote sensing data was carried out using QGIS software. This involved georeferencing (UTM WGS 1984 Zone 44N) and co-registration of multisource data according to the unit grid size of 12.5m×12.5m. Co-registration of the multisource data achieved an accuracy of half per pixel. After the data processing, landslide factor maps and slope facet maps were extracted.

2.2 Methodology

In this study, a modified LHEF rating scheme was adopted for LHZ mapping. Using an empirical evaluation system, the LHEF scheme assigns empirical ratings to various parameters according to their presumed impact on landslides. [20]. Two separate provisions, namely, maximum possible rating values for each factor (Table 2) and a detailed rating scheme for the factor attributes (Table 5), form the building blocks of the LHEF rating scheme. As part of the modification, two external factors, namely, rainfall and seismicity, were incorporated into the rating scheme (Table 3). Following the BIS guidelines, a slope facet was selected as a mapping unit. It has also been adopted by the BIS for carrying out landslide hazard zonation mapping in hilly regions of India. Slope facets are identified on the topographic sheets as per BIS standards. Hence, the quality of the facets lies in the scale and accuracy of the topographic map. Again, the accuracy of topographic maps of highly rugged terrain like the Himalaya is always questionable. Therefore, we have used ALOS PALSAR 12.5m DEM to extract slope facets. From the DEM-derived shaded relief map, facet boundaries (such as ridges, spurs, streams, and rivers) were identified (Fig. 3 a–b). To perform LHZ mapping, 126 slope facets in all were found in the region. For each slope facet, one or more subcategories of factors were assigned ratings following the LHEF scheme. Further, the LHEF rating scheme has the provision of calculating the total estimated hazard value (TEHD) for each slope by using equation 1.

TEHD = LHEF Ratings of [(lithology + structure favorability + slope morphometry + relative relief + LULC + hydrogeological conditions+ External factor) (1)

TEHD for each slope facet was then calculated by adding all the rated sub-categories of the factors present in the individual Slope facets. The TEHD provides a numerical estimate of the degree of landslide propensity for each mapping unit (slope facet), similar to the landslide susceptibility index (LSI). The LHEF scheme allows the TEHD values to be categorized into five relative hazard zones (Table 4). Table 4 presents threshold values that determine the classification of facets into five hazard zones: very low, low, moderate, high, and very high. In the next section we have discussed in detail about the factors and their ratings.

Table 1: List of datasets used in this study

Data Type	Sensor and year	Resolution/Scale	Data Derivative
Multispectral image	Sentinel-2: visible and near-infrared (VNIR) - 2017	10m	Landslide inventory and LULC
	LISS IV: VNIR-2015	15m	Landslide inventory
	WorldView – 2: PAN- 2010	0.5m	landslide inventory
	WorldView – 2: VNIR-2010	1.84m	Photo-lineament and landslide inventory
DEM	ALOS PALSAR	12.5M	Slope Aspect - facet mapping Relative Relief Drainage – hydrogeological conditions
Ancillary Data	Published geology map	1:25000	Digitized Geology map
	Survey of India Toposheet 53 J/7 NW	1:25000	Digitized base map

Table 2: Factors considered under LHEF rating as per BIS Code – IS14496 -2, 1998

Causative factor	Maximum rating scheme
Lithology	2.0
Structure	2.0
Slope Morphometry	2.0
Relative Relief	1.0
Land use and land cover	2.0
Hydrogeological condition	1.0
	Total 10

Table 3: Factors considered under LHEF rating (Modified after Anbalagan2008)

	Landslide causative factors	Maximum LHEF rating
Inherent factors	1. Lithology	2.0
	2. Structure	2.0
	3. Slope parameter a) slope morphometry/angle b) relative relief	2.0
	4. Land use and land cover	2.0
	5. Hydrogeological conditions	1.0
External factors	6 a) Seismicity 6 b) Rainfall	1.0 (=0.5 + 0.5)
	Total	**10.0**

Table. 4: Threshold values recorded in LHEF rating scheme for classifying TEHD values into LHZ

Hazard zone	Range of corrected TEHD value	Description of zone
I	TEHD < 3.5	Very Low Hazard (VLH) zone
II	3.5 ≤ TEHD < 5.0	Low Hazard (LH) zone
III	5.0 ≤ TEHD ≤ 6.5	Moderate Hazard (MH) zone
IV	6.5 < TEHD ≤ 8.0	High Hazard (HH) zone
V	TEHD > 8.0	Very High Hazard (VHH) zone

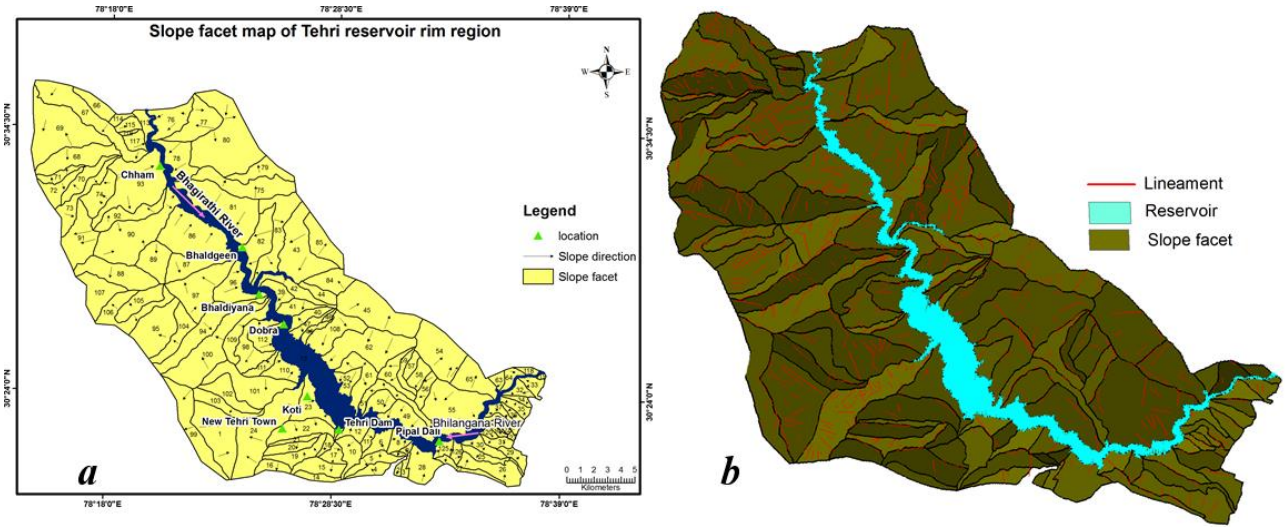

Figure 3 a) slope facet map showing the direction of slope, b) Slope facet based digital terrain model of the study area.

2.2.1 Lithology

The lithology has a major role in regulating the stability of rock slopes, and this category is assigned a maximum LHEF grade of 2. The mass movement's nature is determined by the lithology, and grades are given in accordance with this. Several rock kinds and their state of weathering have been examined throughout the field research. The area's rock formations are shown in Figure 4. The research region mostly consists of two types of rocks: quartzite and phyllite. Table 6 lists the additional lithological units that have been found in the region. These units include of weathered quartzite intercalated with slate, low-grade limestone, alternating bands of quartzite and phyllite, phyllite with small bands of quartzite, and limestone intercalated with slate and siltstone. Phyllites cover the majority of the study area and are exposed to

Table 5 Landslide Hazard Evaluation Factor (LHEF) rating scheme (Source: BIS 14496 Part-2 1998) (-To be continued-)

Contributory factor		Category		Rating
A. Lithology	Rock type	Type– I	Quartzite and limestone	0.20
			Granite an gabbro	0.30
			Gneiss	0.40
		Type – II	Well cemented terrigenous sedimentary rock dominantly sandstone with minor beds of clay stone	1.00
			Poorly cemented terrigenous sedimentary rock dominantly sandstone with minor clay shale beds	1.30
			Slate and phyllite	1.20
		Type – III	Schist	1.30
			Shale with interbedded clayey and non-clayey rocks	1.80
			Highly weathered shale, phyllite, and schist	2.00
	Soil type	Older well compacted alluvial fill material		0.80
		Clayey soil with naturally formed surface		1.00
		Sandy soil with naturally formed surface (Alluvial		1.40
		Debris comprising mostly rock pieces mixed with clayey/sandy soil (Colluvial)		
		Older well compacted		1.20
		Younger loose material		2.00
B. Structure	(i) Relationship of the parallelism between the slope and the discontinuity*	I	>30°	0.2
		II	21°– 30°	0.2
		III	11° –20°	0.3
	Planar (αj-αs)	IV	6° –10°	0.4
	Wedge (αi-αs)	V	<5°	0.5
	(ii) Relationship of dip of discontinuity* and inclination of the slope	I	>10°	0.3
		II	0°– 10°	0.5
		III	0°	0.7
	Planar (βj-βs)	IV	0° – (-)10°	0.80
	Wedge (βi-βs)	V	> (-) 10°	1.00
	(iii) The dip of discontinuity*	I	<15°	0.20
	Planar (βj) Wedge (βi)	II	16°– 25°	0.25
		III	26° –35°	0.30
		IV	36° –45°	0.40
		V	> 45°	0.50
	(iv) The depth of soil cover	I	< 5 m	0.65
		II	6 - 10 m	0.85
		III	11 - 15 m	1.30
		IV	16 - 20 m	2.00
		V	>20 m	1.20

Notes: Correction Factor for Weathering of rock
Highly weathered – Rock discoloured, joints open with weathered products, rock fabric altered to a large extent – correction factors C1; Moderately discoloured with fresh rock patches, weathering more around joint planes, but rock in-tact in nature – correction factor C2; Slightly weathered – Rock along joint planes, which may be moderately tight to open, intact rock – Correction factor C3;
The correction factor for weathering to be multiplied with the fresh rock rating. For Rock Type 1: $C_1 = 4$, $C_2 = 3$, $C_3 = 2$
For Rock Type 2: $C_1 = 1.5$, $C_2 = 1.25$, $C_3 = 1.0$
Discontinuity refers to the planar discontinuity or the line of intersection of two planar discontinuities whichever is important from the point of view of th
α_j = Dip direction of joint ; α_S = Direction of slope inclination ; α_i = Direction of line of intersection of two discontinuities ; β_j = Dip of joint ; β_s = Inclin
Plunge of line intersection of two discontinuities Category I = Very Favourable; II = Favourable; III = Fair; IV = Unfavourable; V = Very Unfavourable

Contributory factor	Category		Rating
C. Slope Morphometry	Escarpment/cliff	=45°	2.0
	Steep slope	36 °– 45 °	1.7

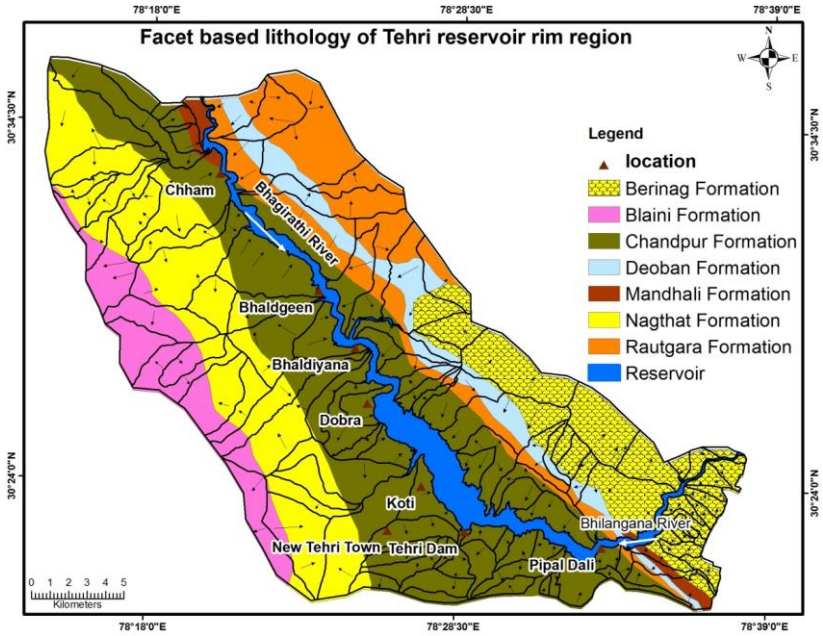

Figure 4 Facet based lithological map of Tehri reservoir rim region (Valdiya 1980)

Table 6: LHEF ratings awarded to rock types represented in Tehri reservoir rim region

S. No.	Formations	Rock type	Gross Ratings
1	Blaini Formation	Quartzite, limestone, slates, phyllites & conglomerate	0.6
2	Berinag Formation	Weathered quartzite intercalated with slate	0.8
3	Nagthat Formation	Weathered quartzite intercalated with slate	1.2
4	Chandpur Formation	Low grade lustrous phyllites	1.4
5	Mandhali Formation	Black carbonaceous pyretic phyllite	0.5
6	Deoban Formation	Dolomitic limestone with phyllitic intercalations	0.8
7	Rautgara Formation	Quartzite, slate, metavolcanic rocks	1

the Bhagirathi River's two banks. In general, these rocks are susceptible to weathering. Quartzite is the second most common type of exposed rock in the research region. Generally hard and compact, these rocks create steep slopes on the region's upper terrain. A dense band of exposed quartzites may be seen spanning from the northwest through the center and up to the southern portion of the region. Comparatively speaking, quartzites with small phyllite bands are weaker than quartzites. The majority of these rocks are visible near the area's center. Phyllites predominate in the northern section, with minor quartzite bands present. These rocks are also exposed on both sides of the Bhagirathi River in the south-eastern corner area. Using BIS (1998) guidelines for the ratings of the rock types, ratings were awarded and are presented in Table 6.

2.2.2 Geological structure

The relationship between the slope's direction and the attitude of the major discontinuities primarily determines the instability of rough terrain made up of in-situ rocks [26]. Primary and secondary discontinuities such as bedding, foliation, schistosity, joints, shear zones, folds, faults, etc. are examples of geological discontinuities. The LHEF rating scheme contains comprehensive criteria (Table 5) to rate the facets with regard to their structural favorability. The scheme requires details of all the discontinuities present on the slope facet, slope inclination, and depth of soil cover (if the slope-forming material is soil, debris, or RBM). Given the extent of the area and the number of slope facets covered, it was not possible to account for the details of the discontinuities present in slope facets. Hence, we have evolved a new method to define the structural favorability of the slope facet. This process involves the following steps: identification of photo-lineaments, computation of the length of photo-lineaments in each facet, calculation of photo-lineament length density for each facet by dividing the total length of photo-lineament within the facet by the area of the facet, and normalizing the density values in the range of 0–2 (recorded in the LHEF rating scheme). In the present study, high-resolution satellite data, including

ALOS PALSAR DEM, was used to extract photolineaments. Linear features such as ridges, spurs, Synclines, faults, and folds were interpreted visually from the high-resolution images (Fig. 5). Lineaments, which were found to be overlapping in two facets, were accounted for in both facets according to their fraction in the slope facet. After the extraction of photo-lineament, photo-lineament length density was calculated, and then it was normalized in the range of 0-2. Further, using the threshold values recorded in the LHEF rating scheme (Table 7), normalized density values were categorized into very favorable, favorable, fair, unfavorable, and very unfavorable classes (Fig. 6).

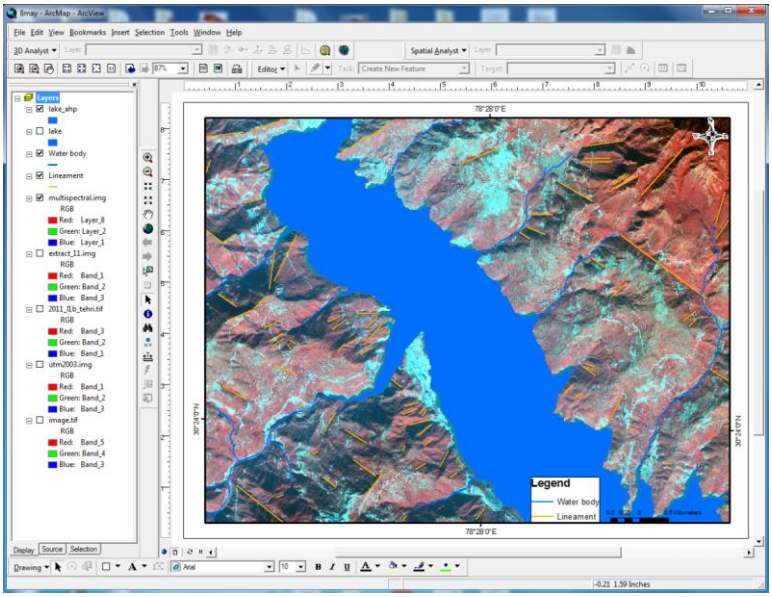

Figure 5 : Procedure of Photo-lineament layer preparation using worlview-2 multispectral image.

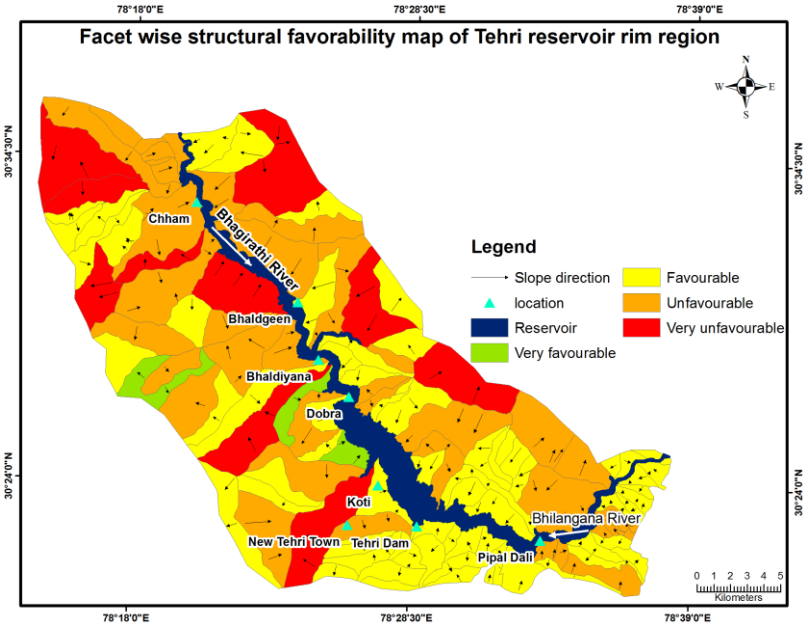

Figure 6 Facet wise structural favorability map of Tehri reservoir rim region

Table 7: Range of structural favorability classes recorded under LHEF rating scheme

Structure Class	LHEF rating (out of 2)	Description
I	Rating ≤ 0.7	Very Favourable
II	0.7 < Rating ≤ 1.05	Favourable
III	1.05 < Rating ≤ 1.4	Fair
IV	1.4 < Rating ≤ 1.75	Unfavourable
V	Rating > 1.75	Very Unfavourable

2.2.3 Slope Parameter

Under the modified LHEF rating system [27], slope parameter is divided into slope angle and relative relief and their combined maximum rating is 2. A matrix-based system was adopted to compute the combined rating of the slope parameter category (Table 8). Details of slope angle and relative relief have been discussed separately in next sub-sections.

a) Slope angle

Facet wise slope map of the area was prepared using the guidelines recorded in LHEF rating system (Fig: 7). DEM was used to compute the slope category of each facet. Continuous raster slope angle data within a particular facet was averaged and the resultant was used as slope angle parameter. Based on threshold value given in LHEF rating scheme (Table 5), continuous slope angle data was categorized in very low, low, moderate, high and very high categories. Maximum rating of 2 is assigned for slope angle in LHEF system.

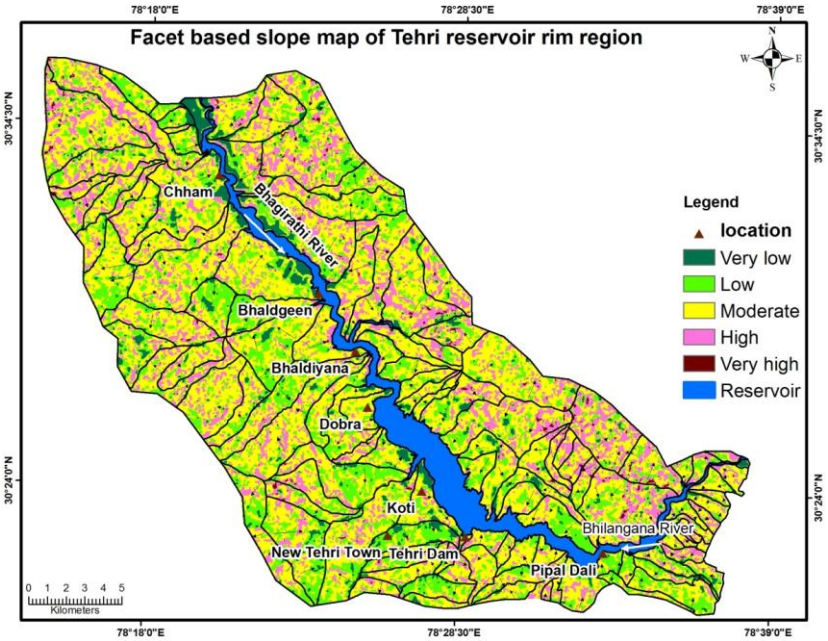

Figure 7: Facet based slope map of Tehri reservoir rim region

b) Relative relief

With a maximum rating of 1, relative relief is defined as the difference between the slope facet's maximum and minimum elevations. Figure 8 is the relative relief map of the research area, and Table 5 lists the various classes of relative relief taken into account in the LHEF rating methodology. In this work, we used modified LHEF ratings for the slope parameter. We combined the slope angle and relative relief in order to get a maximum rating of 2. The combination of slope angle and relative relief rating value was determined by setting a matrix form (5×5) in which slope angle was kept in rows and relative relief was kept in columns (Table 8). The LHEF ratings increase from left to right in rows, while they decrease from top to bottom in columns. This reflects that, out of the two factors, slope morphometry is given more weight over relative relief. As per the fit of the extracted slope angle and relative relief classes, ratings of the slope parameters were assigned and found to vary in a range of 0.50 to 1.8.

Table 8: Matrix adopted for awarding ratings to slope parameters under LHEF rating scheme

Slope parameter		a) Slope morphometry classes				
		A (< 15º)	B (16–25°)	C (26-35°)	D (36-45°)	E (> 45°)
b) Relative relief classes	I (< 50m)	0.5	0.9	1.3	1.5	1.8
	II (50 -100m)	0.6	1.0	1.4	1.6	1.9
	III (101-200m)	0.7	1.1	1.5	1.7	1.95
	IV (201-300m)	0.8	1.2	1.55	1.75	2.0
	V (> 300m)	0.9	1.3	1.6	1.8	2.0

2.2.4 Land use/land cover

The entire region was divided into five LULC classes: water bodies, dense forests, scrub forests, agricultural land, and settlements (Fig. 9). The LHEF grading scheme was used to assign ratings to the LULC categories (Table 9). In the event that a single slope facet contains multiple LULC pattern types, the LHEF rating of the facet is obtained by multiplying the fraction area of each LULC pattern by its associated rating and adding the results.

2.2.5 Hydrogeological condition

In steep terrain, ground water often follows weak rock planes rather than following a consistent pattern. Large-scale observational examination of the behavior of ground water on hill slopes is not feasible [20]. For LHZ mapping, surface expression of ground water was taken into consideration in order to expedite the assessment process. Surface indication of ground water such as flowing, dripping, wet, damp and dry is recorded in LHEF rating scheme. To assess the probability of worst hydrogeological condition, post monsoon terrain observation was considered for the rating. In case of slope facets showing wet, damp and dry conditions, the dominant type of hydrogeological conditions were assessed and the rating awarded. The fractional ratings were calculated to get the total LHEF rating for each slope facet.. Three hydrogeological conditions namely, dry, dry to damp and damp were observed on the basis of their surface expressions (Fig: 10) and assigned ratings accordingly (Table 10).

Table 9: LHEF ratings values calculated for land use/land cover classes

LULC classes	Rating
Agricultural land	0.65
Dense forest area	0.80
Scrub forest area	1.50
Settlement/ barren land	1.70

Table 10: LHEF ratings calculated for hydrogeological conditions classes

Hydrogeological condition on slope	Rating
Dry	0.0
Dry to damp	0.1
Damp	0.2

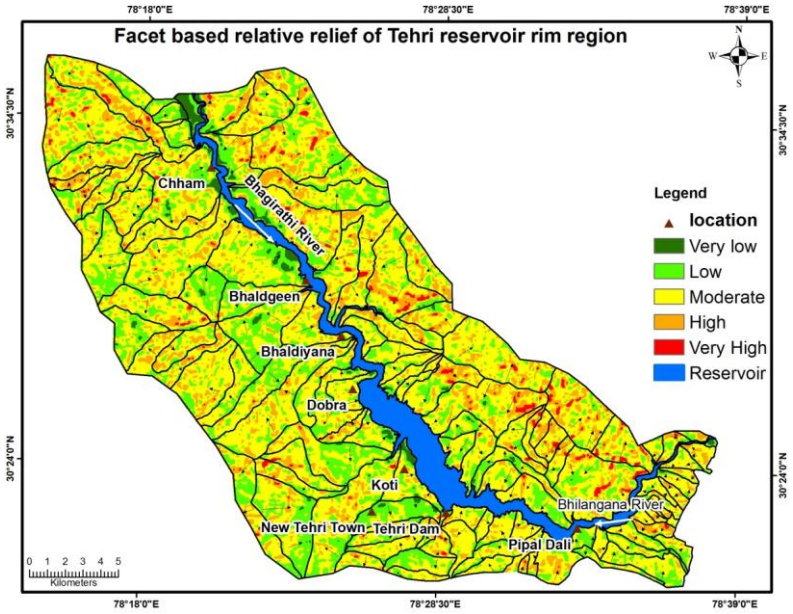

Figure 8 Facet based relative relief map of Tehri reservoir rim region

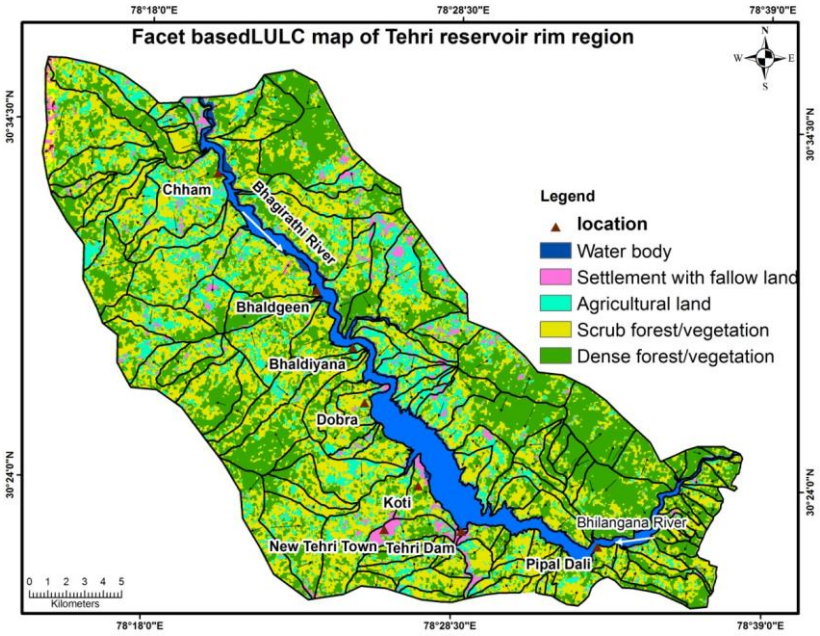

Figure 9 Facet based LULC map of Tehri reservoir rim region

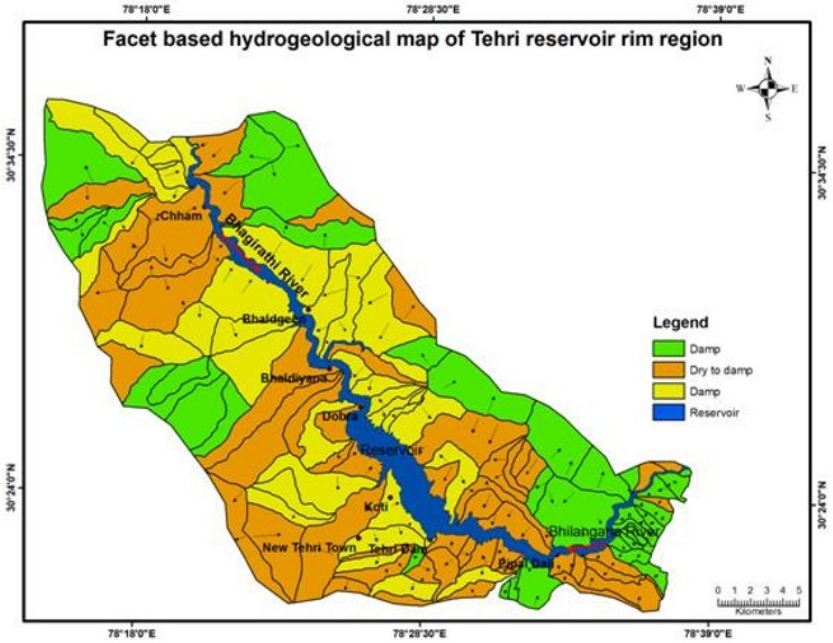

Figure 10 Facet based hydrogeological map of Tehri reservoir rim region

2.2.6 External Factors

External factors such as earthquakes and rainfall can induce landslides and are called triggering factors. Their effect is conspicuous over a large area and it is obvious that their effect will not vary from facet to facet (Anbalagan et al. 2008). A slope facet which is stable under current slope situation might become instable if it falls under high earthquake prone or high precipitation zone and may result in landslide phenomenon. Following an intense precipitation, chances of abrupt increase in pore water pressure becomes inevitable. Slope facets owing to high pore water pressure may also induce landslides. It is understandable that in case of a slope facet falling in high annual precipitation zone and also high earthquake activity (as in the case of Himalaya); propensity of landslide hazard may get enhanced. Maximum rating of 1 is awarded to the external factors and is equally divided between seismicity and rainfall. The present study area falls under seismic zone-IV (BIS 2002) and also receives moderate to high precipitation uniformly throughout the area hence a rating of 0.8 was awarded to each facet.

2.2.7 Data Integration and TEHD

TEHD reflects the general situation of instability of a terrain and is computed for each facet by adding the LHEF ratings of inherent parameters and external parameters (Equation 1). The calculated TEHD value can vary widely between different facets depending on the condition of instability of the respective facets [28]. TEHD In this case, TEHD values were found to be varying between 4.45 to 7.6 (Fig: 11).

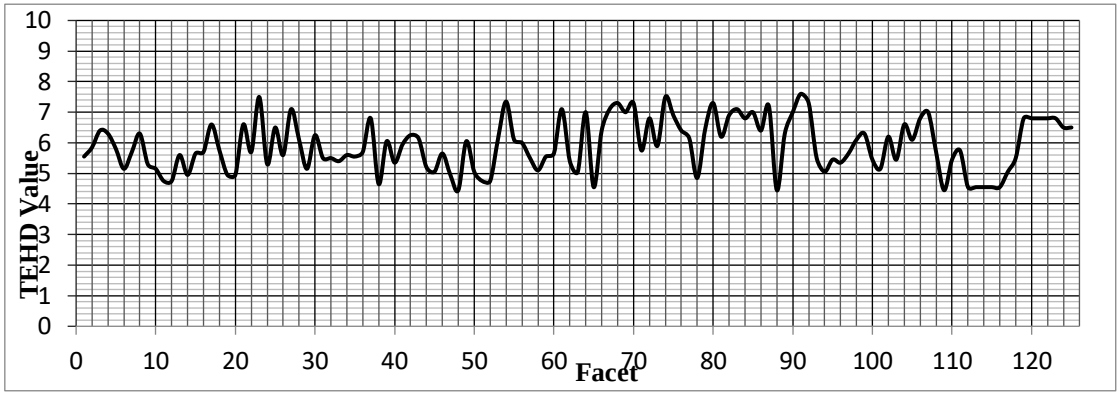

Figure 11 Frequency of TEHD value calculated for each facet.

Based on the facets' computed TEHD values, the current area's LHZ map is created (Fig:12). The LHEF scheme uses threshold values to classify the range of TEHD values into five relative hazard zones (Table 4). The physical distribution of these danger zones is depicted on the LHZ map, which aids planners in choosing comparatively safe locations for upcoming development-related projects.

3. Results and Discussion

LHZ mapping based on the modified LHEF rating scheme has been carried out, and the results generally match the ground physical conditions. The extraction of slope facets through the combination of visual and digital image interpretation has resulted in the accurate demarcation of slope facets. A 3D model of the slope facet (Fig. 2b) produced using geospatial tools accurately represents the field condition. When compared to other relevant work [17, 20, 26–28], the slope facet produced in the present work makes more sense. A major challenge has been the identification of the structural favorability of slopes. In this work, a methodology was evolved to extract structural favorability information by using photo-lineament density. It can make quick appraisals of structural information and is better suited for macroscale mapping. The LHEF scheme only incorporates inherent landslide-causing factors and thus omits important external factors, namely rainfall and seismicity. For conditions like Himalaya, where rainfall and seismic activities are intense, the inclusion of external factors would result in better prediction. In this work, external factors were included and relevant ratings were proposed. Additionally, a matrix system proposed by [26] was used to rate an important slope morphometry parameter, relative relief. By combining the ratings of each factor, TEHD was calculated and reclassified into five relative landslide hazard zones following BIS guidelines. Provision for the validation of the LSZ map is not proposed in the BIS code. Several methods, such as the success rate curve, prediction rate curve, receiver operating characteristic (ROC) curve, etc., are frequently used for the accuracy assessment of the LHZ results. These are based on landslide training and testing data, making them suitable for statistical and machine learning methods. The empirical rating scheme used in this work does not include landslide inventory for training or testing purposes. Thus, a comparison was made between the slope facets, LHZ classes, and existing landslide inventory to validate the method (Fig. 13). The bar diagram in Figure 13 shows that 14.2% of the study area falls under the high hazard zone, which contains 21% of the landslide inventory and generally complies with the field conditions. The moderate hazard zone contains 39% of the entire study area and 47.4% of the landslide inventory. The low-hazard zone occupies almost 40% of the study area and 23.7% of the total landslides. Such a high percentage of landslides in low-hazard zones can be attributed to anthropogenic activities. The very low-hazard zone occupies 7.7% of the study area and occupies almost 8% of the total landslides observed. A very high-hazard zone is not found on the LHZ map.High hazard slope facets are mostly reflected at places where the terrain is steep, relative relief is high and lithology is phyllitic in nature. These areas also support open/scrub forest and high drainage density. Out of the 126 slope facets, 21 falls under high hazard zone category and majority of high hazard slope facets (14) are making side slopes of the reservoir. Moderate hazard zones are found all over the area and are associated with gentle slopes, moderate relative reliefs and agricultural areas. Slope facets, which come under low and very low hazard zones are found to be associated with the densely forested area, agricultural area, terrace and gentle talus slopes.

A comparative analysis revealed that about 69% of all landslides and 53.5% of all aspects are located in high and moderate danger zones. Nearly 46.5% of the aspects are in very low and low hazard zones, with 31% of landslides. Using this strategy, a very high hazard zone was not detected. Based on the comparison, it can be concluded that the LHZ mapping techniques have identified landslide-prone locations with a respectable degree of accuracy.

4. Conclusions

In this work, an attempt was made to utilize a modified LHEF rating scheme to delineate the landslide hazard zones of the slopes bounding the Tehri reservoir at the macroscale. The mapping unit'slope facet' was precisely identified by using the capabilities of geospatial techniques. Geoenvironmental factors recorded in the LHEF scheme were extracted using a combination of ancillary data and satellite data. A certain degree of modification was made in the LHEF rating

scheme to accommodate structural discontinuity (photo-lineament) and external factors (rainfall and seismicity). Given the extent of the area and number of facets covered, it was not possible to account for the details of structural discontinuities present in slope facets; thus, photo-lineament length density was used to evolve the rating criteria under the structural favorability class. External factors, such as rainfall and seismicity, were also included in the rating scheme. In order to accommodate the external factors in the LHEF rating scheme, slope morphometry parameters (slope angle and relative relief) were merged, and a matrix-based rating system was used for the slope morphometry class.

The final LHZ map showed very promising results, as a high density of landslides was observed in moderate to high hazard zones. A comparison was made between the relative hazard zones, slope facets, and existing landslide inventory. It showed that high and moderate hazard zones occupied 53.5% of the total facets and almost 69% of the total landslides, whereas very low and low hazard zones occupied almost 46.5% of the facets and 31% of the total landslides. This comparison confirmed the robustness of the modified LHEF scheme in identifying relative hazard zones. Though ample work on LHZ mapping is available for Himalaya, almost none of them is given attention by the planners, mainly due to the choice of mapping unit and applied method. In this work, we have simplified the mapping unit problem by adopting a precise slope facet and modified the LHEF rating scheme so that a quick appraisal of landslide hazard conditions can be made, and thus planners can aptly use this map for landslide hazard mitigation.

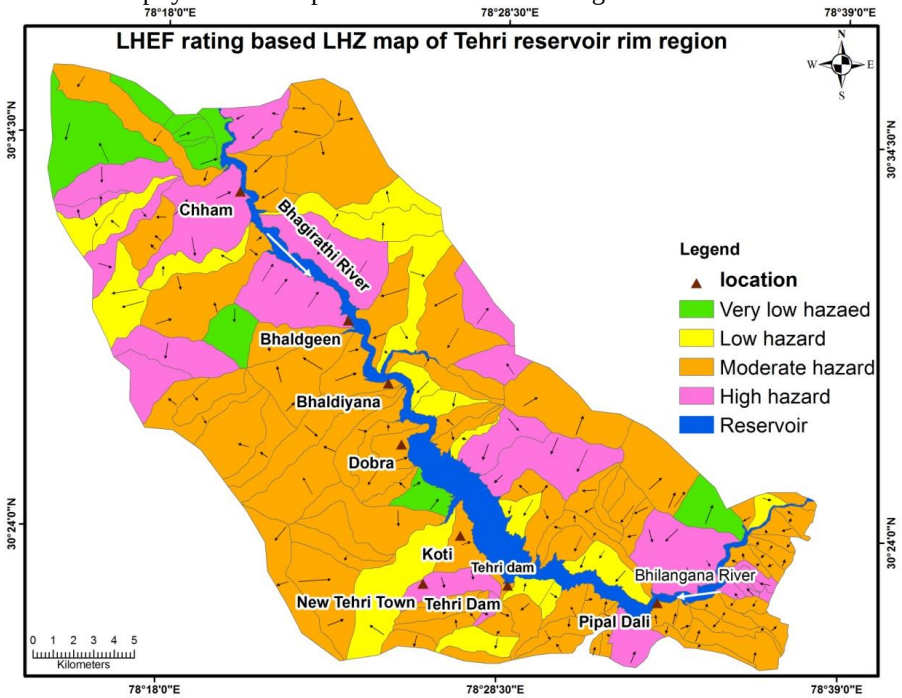

Figure 12 LHEF rating based LHZ map of Tehri reservoir rim region

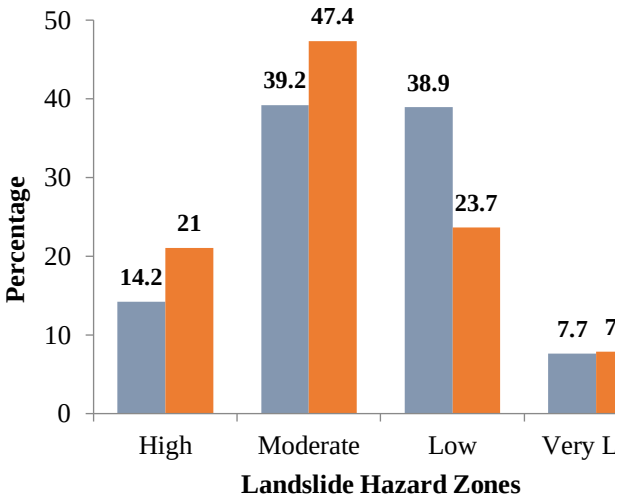

Figure 13 Bar diagram representing percentage domain of relative hazard zone with respect to associated percentage domain of landslide occurrences

References

[1] R Kumar and R Anbalagan. 'Landslide susceptibility mapping of the Tehri reservoir rim area using the weights of evidence method'. Journal of Earth System Science 128(6) (2023): 1-18.

[2] K Khusulio and R Kumar. 'Feasibility assessment of multi-criteria decision making and quantitative landslide susceptibility methods: A case study of Mao-Maram Manipur' Journal of Earth System Science 132(2)(2023) : 56

[3] S Mani and SE Saranaathan, 'Landslide hazard zonation mapping on meso-scale in SH-37 ghat section, Nadugani, Gudalur, the Nilgiris, India'**.** Arabian Journal of Geosciences 10(161)(2017) https://doi.org/10.1007/s12517-017-2932-1

[4] QB Pham, Y Achour, SA Ali, F Parvin, M Vojtek, J Vojteková & D T Anh. 'A comparison among fuzzy multi-criteria decision making, bivariate, multivariate and machine learning models in landslide susceptibility mapping'. Geomatics, Natural Hazards and Risk, 12(1) (2021) 1741-1777.

[5] C Carabella, J Cinosi, V Piattelli, P Burrato, & E Miccadei. 'Earthquake-induced landslides susceptibility evaluation: A case study from the Abruzzo region (Central Italy)'. Catena, 208 (2022) 105729.

[6] N Boukhres, M Mastere, Y Thiery, O Maquaire, B El Fellah and S Costa. 'A comparative modeling of landslides susceptibility at a meso-scale using frequency ratio and analytic hierarchy process models in geographic information system: the case of African Alpine Mountains (Rif, Morocco)'. Modeling Earth Systems and Environment, 9(2)(2023) : 1949-1975.

[7] R Kumar and R Anbalagan. 'Landslide susceptibility zonation in part of Tehri reservoir region using frequency ratio, fuzzy logic and GIS'. Journal of Earth System Science 124(2) (2015) : 431-448.

[8] RP Riegel, DD Alves, BC Schmidt, GG de Oliveira, C Haetinger, DMM Osório and DM de Quevedo, 'Assessment of susceptibility to landslides through geographic information systems and the logistic regression model'. Natural Hazards 103(1)(2020) : 497-511.

[9] ER Sujatha and V Sridhar. 'Landslide susceptibility analysis: a logistic regression model case study in Coonoor, India'. Hydrology 8(1)(2021) : 41

[10] K Khusulio and R Kumar. 'Landslide impacting factors and susceptibility assessment in part of the Purvanchal Himalayas using data mining approaches '. Arabian Journal of Geosciences 16(11)(2023) : 612

[11] A Singh, S Pal, DP Kanungo. 'An integrated approach for landslide susceptibility–vulnerability–risk assessment of building infrastructures in hilly regions of India'. Environment, Development and Sustainability 23(4)(2021) : 5058-5095.

[12] L Shano, TK Raghuvanshi and M Meten. 'Fuzzy set theory and pixel-based landslide risk assessment: the case of Shafe and Baso catchments, Gamo highland, Ethiopia'. Earth Science Informatics 15(2)(2022) : 993-1006.

[13] NA Shah, M Shafique, M Ishfaq, K Faisal and M Van der Meijde. 'Integrated Approach for Landslide Risk Assessment Using Geoinformation Tools and Field Data in Hindukush Mountain Ranges, Northern Pakistan'. Sustainability 15(4)(2023) : 3102

[14] H Wang, G Long, J Liao, Y Xu and Y Lv. 'A new hybrid method for establishing point forecasting, interval forecasting, and probabilistic forecasting of landslide displacement'. Natural Hazards (2022) 1-27.

R Anbalagan 'Landslide hazard evaluation and zonation mapping in mountainous terrain'. Engineering Geology 32(1992) : 269–277.

[15] A Sajwan, S Mhaski, A Pandey, P Vangla and GV Ramana. 'A multi-scale approach for deterministic analysis of landslide triggering and mass flow mechanism at Kaliasaur (Rudraprayag)'. Landslides (2023) 1-17.

[16] D Sun, S Shi, H Wen, J Xu, X Zhou, and J Wu. 'A hybrid optimization method of factor screening predicated on GeoDetector and Random Forest for Landslide Susceptibility Mapping'. Geomorphology, 379(2021) : 107623.

[17] A Arabameri, S Chandra Pal, F Rezaie, R Chakrabortty, A Saha, T Blaschke and PT Thi Ngo. 'Decision tree based ensemble machine learning approaches for landslide susceptibility mapping'. Geocarto International 37(16)(2022) : 4594-4627.
[18] A Tyagi, RK Tiwari and N James. 'A review on spatial, temporal and magnitude prediction of landslide hazard'. Journal of Asian Earth Sciences (2022) X. https://doi.org/10.1016/j.jaesx.2022.100099

[19] S Liu, L Wang, W Zhang, Y He and S Pijush. 'A comprehensive review of machine learning-based methods in landslide susceptibility mapping. Geological Journal (2023) https://doi.org/10.1002/gj.4666

[20] R Anbalagan, D Chakraborty and A Kohli. 'Landslide hazard zonation (LHZ) mapping on meso-scale for systematic town planning in mountainous terrain'. Journal of Scientific & Industrial Research 67(2008) : 486-497.

[21] P Gupta and R Anbalagan. Landslide hazard zonation (LHZ) and mapping to assess slope stability of parts of the proposed Tehri dam reservoir, India. Quarterly Journal of Engineering Geology and Hydrogeology, 30(1997) : 27-36

[22] J Saleem, SS Ahmad and A Butt. 'Hazard risk assessment of landslide-prone sub-Himalayan region by employing geospatial modeling approach'. Natural Hazards, 102(2020) : 1497-1514.

[23] DD Pandey, RS Banshtu, K Singh. 'Landslide Hazard Assessment Along Lahru to Chamba, Himachal Pradesh, India, Using Certainty Factor Approach'. In Sustainable Development Through Engineering Innovations: Select Proceedings of SDEI 2020 (pp. 73-84). Springer Singapore.

[24] RK Panigrahi and G Dhiman, 'Risk Assessment and Early Warning System for Landslides in Himalayan Terrain. In Stability of Slopes and Underground Excavations' Proceedings of Indian Geotechnical Conference 2020 Volume 3 (pp. 23-32). Springer Singapore.

[25] KS VALDIYA 'Geology of Kumaun Lesser Himalaya'. Dehradun: Wadia Institute of Himalayan Geology. Interim. Report (1980) pp ; 291

[26] D Chakraborty and R Anbalagan. 'Landslide hazard evaluation of road cut slopes along Uttarkashi–Bhatwari road, Uttaranchal Himalaya'. Journal of Geological Society of India 71(2008) : 15–124.

[27] R Anbalagan, D Chakraborty and A Kohali. 'A Landslide hazard zonation (LHZ) mapinh on meso-scale for systematic town planning in mountainous terrain'. Journal of Scientific and Industrial Research 67(2008): 486-497.

[28] M Kannan, E Saranathan and R Anbalagan. 'Comparative analysis in GIS-based landslide hazard zonation – a case study in Bodi-Bodimettu Ghat section, Theni District, Tamil Nadu, India'. Arabian Journal of Geosciences 8(2014) : 691–699.

.

.